Development of a LC-MS/MS method to measure serum 3-sulfate and 3-glucuronide 25-hydroxyvitamin D3 metabolites; comparisons to unconjugated 25OHD in pregnancy and polycystic ovary syndrome

Huynh, Khanh; Kempegowda, Punith; Tamblyn, Jennifer; O'Reilly, Michael; Mueller, Jonathan Wolf; Hewison, Martin; Jenkinson, Carl

DOI:
10.1016/j.steroids.2021.108812

Document Version
Peer reviewed version

Citation for published version (Harvard):
Huynh, K, Kempegowda, P, Tamblyn, J, O'Reilly, M, Mueller, JW, Hewison, M & Jenkinson, C 2021, 'Development of a LC-MS/MS method to measure serum 3-sulfate and 3-glucuronide 25-hydroxyvitamin D3 metabolites; comparisons to unconjugated 25OHD in pregnancy and polycystic ovary syndrome', *Steroids*, vol. 169, 108812. https://doi.org/10.1016/j.steroids.2021.108812

Development of a LC-MS/MS method to measure serum 3-sulfate and 3-glucuronide 25-hydroxyvitamin D3 metabolites; comparisons to unconjugated 25OHD in pregnancy and polycystic ovary syndrome

K. Huynh[1], P. Kempegowda[1], J. Tamblyn[1], M.W. O' Reilly[1], J.W. Mueller[1], M. Hewison[1], C. Jenkinson[1].

[1]Institute of Metabolism and Systems Research, University of Birmingham, Birmingham, UK.

Short title

LC-MS/MS measurement of 3-sulfate and 3-glucuronide 25-hydroxyvitamin D3 metabolites

Correspondence: Dr Carl Jenkinson

Institute of Metabolism and Systems Research

University of Birmingham

Wolfson Drive, Birmingham, Edgbaston, B15 2TT, United Kingdom

Email: C.Jenkinson@Bham.ac.uk

Abstract

Vitamin D status is routinely assessed by measuring circulating concentrations of 25-hydroxyvitamin D ($25OHD_2$ or $25OHD_3$). However as deconjugation is not routinely incorporated into sample treatment prior to analysis, conjugated forms of 25OHD (particularly the more abundant $25OHD_3$) are often not considered in determining serum concentrations of total 25OHD. Two major circulating conjugated forms of $25OHD_3$ are 25-hydroxyvitamin $_{D3}$-3-sulfate ($25OHD_3$-S) and 25-hydroxyvitamin $_{D3}$-3-glucuronide ($25OHD_3$-G). Incorporating these two conjugated metabolites into the measurement of vitamin D status could improve our understanding of vitamin D status in health, particularly if there are changes in sulfation and glucuronidation activities. The aim of this study was to develop a liquid chromatography tandem-mass spectrometry (LC-MS/MS) targeted method for measurement of $25OHD_3$-S and $25OHD_3$-G in serum to enable comparisons with circulating levels of the free $25OHD_3$ form. We developed and validated a new LC-MS/MS method that measured both $25OHD_3$-S and $25OHD_3$-G following a solid phase extraction sample preparation method. Partial separation of analytes by LC, and the separation of analytes by the optimized multiple reaction monitoring transitions enabled the quantitation of both 25OHD3-S and 25OHD3-G in the single method. Serum concentrations of $25OHD_3$-S (24.7 ± 11.8 ng/mL) and $25OHD_3$-G (2.4 ± 1.2 ng/mL) were shown to be a significant proportion of circulating vitamin D metabolites in healthy donor serums. These levels of $25OHD_3$-S and $25OHD_3$-G closely associated with $25OHD_3$ concentrations, r=0.728, p=0.001 and r=0.632, p=0.006 respectively. However in serum from pregnant women and non-pregnant women with polycystic ovary syndrome (PCOS) significant differences in the ratios between conjugated and free $25OHD_3$ were observed between pregnancy groups ($25OHD_3$/$25OHD_3$-S and $25OHD_3$/$25OHD_3$-G $p<0.001$), and between healthy and PCOS subjects ($25OHD_3$/$25OHD_3$-G $p<0.050$). Development of this novel high-throughput LC-MS/MS method indicates that $25OHD_3$-S and $25OHD_3$-G are substantial components of circulating vitamin D metabolites. The concentrations of these metabolites relative to conventional $25OHD_3$ may vary in different physiological and pathophysiological settings, and may therefore play an unrecognized but important role in the actions of vitamin D.

Keywords

Vitamin D, Conjugation, LC-MS/MS, Method development, Pregnancy, PCOS.

1. Introduction

Vitamin $_{D3}$ is produced from 7-dehydrocholestorol following UV radiation of skin. Then two-step hydroxylation generates the vitamin D receptor (VDR)-binding metabolite 1,25-dihydroxyvitamin $_{D3}$ ($1,25(OH)_2D_3$) (1-3). The first metabolite formed from vitamin D by the action of the enzyme vitamin D-25-hydroxylase (CYP2R1 and CYP27A1) (4, 5) is 25-hydroxyvitamin D_3 ($25OHD_3$), the most abundant serum metabolite of vitamin D. Because of its long half-life and high abundance in circulation, the serum measurement of 25OHD (combining $25OHD_3$ and $25OHD_2$) is currently considered to be the most reliable estimation of vitamin D status for any given individual, even though $25OHD_3$ is not the biologically active form of vitamin D (6, 7).

Phase I metabolism of vitamin D includes the hydroxylation of $25OHD_3$ by CYP27B1, primarily in the kidney but also at specific extra-renal sites, forming hormonally active $1,25(OH)_2D3$ (8). In addition, 25OHD can undergo a series of other metabolic reactions including catabolic inactivation by 23- and 24-hydroxylation and C3-epimerization (3). As well as these phase I metabolic reactions, $25OHD_3$ undergoes phase II conjugation by sulfation and glucuronidation. The phase I pathway for activation of vitamin D and phase II metabolic pathways of 25OHD3 are shown in Figure 1, adapted from a comprehensive review of vitamin D metabolism by Jenkinson *et al.*(3).

Two UPD-glucuronosyltransferase (UGT) enzymes, UGT1A4 and UGT1A3 have demonstrated conjugating activity for $25OHD_3$, forming three glucuronide metabolites; $25OHD_3$-3-G, $25OHD_3$-25-G (9). Also following 5,6-trans-$25OHD_3$ conversion from $25OHD_3$, the glucuronide metabolite 5,6-trans-$25OHD_3$-25-G can be been formed in UGT1A4/UGT1A3 human liver microsomes (9, 10). Glucuronidation of $25OHD_3$ at carbon position 3 ($25OHD_3$-G) and position 25 ($25OHD_3$-25G) has also previously been reported in rat bile (11). $25OHD_3$-3G, the major glucuronide metabolite measured in human plasma and bile, has been reported in circulation at low nM concentrations (9, 12). The 3-glucuronide metabolite has also been measured as a urinary excreted metabolite (13). Interindividual variations in glucuronidation activity of $25OHD_3$ may occur and a variant in the gene polymorphism of UGT2A1 alters the rate of $25OHD_3$ glucuronidation (9).

The major circulating sulfated 25OHD$_3$ metabolite is 25OHD$_3$-3-sulfate (25OHD$_3$-S) which has previously been measured in circulation at levels similar to that of 25OHD$_3$ (12, 14-16). Sulfotransferase SULT2A1 has been identified as the major sulfating enzyme of 25OHD$_3$, as well as other vitamin D metabolites (17-19). The SULT1A1 or SULT2B1a/b enzymes do not have sulfation activity towards 25OHD$_3$, however these SULT enzymes have shown activity for sulfation of calcitriol and 7-dehydrocholesterol respectively (17, 19). This has led to the hypothesis that the vitamin D$_3$-S could be hydroxylated to form 25OHD$_3$-S (19). The sulfation rate of 25OHD$_3$ by SULT2A1 varies between individuals based on a single nucleotide variant of SULT2A1 (18).

The biological roles of 25OHD$_3$-G and 25OHD$_3$-S and their contribution to 25OHD status are still not fully understood, despite 25OHD$_3$-S being identified in circulation as early as 1985 (20). One hypothesis suggests that reduced renal elimination enables higher concentrations of the conjugated 25OHD$_3$ metabolites in circulation. In this way, 25OHD$_3$-G and 25OHD$_3$-S could serve as a reservoir for 25OHD$_3$ through deconjugation to 25OHD$_3$, particularly at target tissue sites (3, 12, 16, 18). Analysis of conjugated 25OHD$_3$ metabolites, along with free 25OHD$_3$ measures could therefore be important in providing a more comprehensive assessment of vitamin D status, particularly in different disease states in which conjugation and hydrolysis activity may be altered.

Previous studies have reported methods using liquid chromatography (LC) coupled to ultraviolet detection (UV) or mass spectrometry (MS) for measuring 25OHD$_3$-S (14, 15, 21, 22) or 25OHD$_3$-G (9). A recent method has described a simultaneous method to measure both 25OHD$_3$-S and 25OHD$_3$-G in circulation. However, this method required derivatization for reliable detection of the 25OHD$_3$-G analyte (12). There is also limited knowledge on the clinical role of vitamin D conjugation, as measurements and the ratios between conjugated 25OHD$_3$ and the free form have not previously been reported for different health and disease groups.

The aim of this study was to develop an ultra-performance liquid chromatography tandem-mass spectrometry (UPLC-MS/MS) method to measure 25OHD$_3$-S and 25OHD$_3$-G in a single sample run, without the need for derivatization, suitable for high throughput. Using our method, we wanted to compare sulfated, glucuronidated and free 25OHD$_3$ in pregnancy, where changes in vitamin D metabolism and metabolite levels have been previously associated with pregnancy

outcomes (23). We finally set out to specifically analyse $25OHD_3$-S and $25OHD_3$-G, along with free $25OHD_3$ in patients with polycystic ovary syndrome (PCOS), where vitamin D-deficiency has been previously linked to with PCOS (24).

2. Experimental

Materials

$25OHD_3$-S, $25OHD_3$-S-(26,26,26,27,27,27)d6 and $25OHD_3$-G were purchased from Toronto Research Chemicals (Toronto, Canada). $25OHD_3$, LC-MS grade methanol, water and acetonitrile were purchased from Sigma Aldrich (Poole, UK). Oasis HLP solid phase extraction (SPE) cartridges were purchased from Waters Corporation (Manchester, UK). Vitamin D depleted serum was purchased from Golden West Biologicals (Temecula, California, USA).

Sample collection

Pregnancy and healthy control serum sample collection and ethical approval has been described previously (NHS REC approval 06/Q2707/12 and 13/WM/0178 [2014–2024]) (23). Women with PCOS aged between 18 and 40 years were recruited from outpatient clinics at University Hospitals Birmingham and Birmingham Women's Hospital as previously reported (25) Exclusion criteria for the study were as follows: recent glucocorticoid treatment (within 3 months), pregnancy, age younger than 18 or older than 45 years, recent oral contraceptive use (within 3 months), hyperprolactinemia, thyroid disorders, and dysglycemia (impaired fasting glucose, impaired glucose tolerance or overt diabetes mellitus). PCOS women were also excluded if they had received prior treatment with metformin, insulin sensitizers or androgen receptor blockers. Full ethical approval was obtained from Edgbaston Research Ethics Committee (reference 12/WM/0206) and all participants provided written informed consent prior to inclusion in the study. PCOS was diagnosed according to the Rotterdam European Society of Human Reproduction and Embryology (ESHRE) 2004 criteria, with the presence of two or more of the following: oligo/anovulation (Anov), clinical signs of androgen excess (AE), and polycystic ovaries (PCO) on ultrasound (26); however, only PCOS women with clinical or biochemical signs of androgen excess were recruited to the *in vivo* study (phenotypes AE+Anov+PCO, AE+Anov and AE+PCO). Other potential causes of oligomenorrhea and androgen excess were excluded by history, physical examination and biochemical assessment. All healthy controls were age- and BMI-matched, and recruited via local advertisement, with exclusion of PCOS on clinical and biochemical grounds. Baseline serum samples for LC-MS/MS were taken at 9am, where possible in the early follicular phase; in the setting of oligo- or amenorrhoea samples were taken randomly.

Sample preparation

Samples were prepared by solid phase extraction following protein precipitation based on a previously described method (21). Briefly, 20 µL serum was precipitated with 50 µL acetonitrile containing 8 ng/mL 25OHD$_3$-S-d6 internal standard. Samples were vortexed and centrifuged at 1000 x g for 10 minutes. Sample supernatants were diluted with 300 µL water and adsorbed on to Oasis HLB cartridges by applying a vacuum followed by washing through with 1 mL water and 1 mL methanol/water (1:1 v/v). Samples were eluted from these cartridges with 1 mL methanol. Eluted samples were dried down and reconstituted with 100 µL water/methanol (1/1 v/v) for injection by LC-MS/MS.

LC-MS/MS

Mass spectrometry analysis was performed on a Waters AQCUITY UPLC chromatography system coupled to a Waters Xevo TQ-XS mass spectrometer, using electrospray ionization in negative mode. Analytes were quantified by optimizing multiple reaction monitoring (MRM) transitions of each analyte, using full scans and daughter scans as well as manual infusion of each analyte. The optimized MRM transitions for each analyte is shown in **Table 1**. The optimum MS parameters were: desolvation temperature 500 ^{o}C, source temperature 150 ^{o}C, capillary voltage 2.90 kV and cone voltage 100 V. A Waters UPLC BEH C18 (2.1 x 50 mm, 1.7 µm) column was used for separation of metabolites by liquid chromatography. The mobile phase was water-A/methanol-B containing 0.1% formic acid. A 20 µL injection volume was used for injecting the sample into the LC-MS/MS. The total run time was 4.5 minutes with a mobile phase gradient; 0-0.50min: 50%-A:50%-B, 2.00-2.50min: 5.0%-A:95%-B, 3.00-4.00min: 50%-A:50%-B.

Table 1. Optimised MRM transitions

Compound	Mass to charge ratio (m/z)		Cone voltage (V)	Collision energy (eV)
25OHD$_3$-S	479.4	79.8 96.9 122.9	40 40 40	80 32 60
25OHD$_3$-G	575.4	74.9 84.9 122.9	50 50 50	34 40 30
25OHD$_3$-S-d6	485.4	79.8 96.9 122.9	40 40 40	76 34 70

Data analysis

Calibration curves and quantification of data to determine sample concentrations was performed using Waters Target Lynx software. Calibration curves were generated by plotting the peak area ratio of the analyte over the area of internal standard against the respective analyte concentration of each calibrant. A weighing of 1/x was used for plotting the calibration curve regression.

SPSS Statistics Software was used to for statistical tests. Pearson correlation was used to compare correlation trends between analytes. One way ANOVA and independent T-Tests were performed to compare analyte concentrations and ratios between sample groups.

Method Validation

The analytical method was validated based on FDA guidelines (27) for the assessment of selectivity, accuracy, precision, lower limits of detection (LOD) and quantification (LLOQ). Quality control samples for validation were prepared by spiking known concentrations of analytes in vitamin D depleted serum and extracted and analysed in the same manner as unknown serum samples.

The selectivity of the method was confirmed by determining no detectable interfering signals could be observed at the retention times of 25OHD$_3$-S, 25OHD$_3$-G and 25OHD$_3$-S-d6. Three MRM transitions were monitored for each analyte, with two qualifier ions used to enhance specificity. Selectivity was further tested by injecting vitamin D depleted serum spiked with known concentrations of 25OHD$_3$-S and 25OHD$_3$-G and monitoring the MRM chromatograms of each analyte.

Inter-day accuracy, along with intra-day and inter-day precision was determined at three concentration quality control (QC) levels that were distributed based on high, medium and low levels across an expected linear reference range. Accuracy was calculated by the mean calculated value of six replicate sample concentrations at each QC level. Precision was determined by the mean value of six replicates across each QC level (Intra-day) and the mean value of six replicates each day for three consecutive days for each QC level (Inter-day). The LOD and LLOQ were determined by defining the lowest concentration that could be accurately quantified with an analyte response that gave a signal to noise ratio of at least 3 (LOD) and 10 (LLOQ).

Application of the method to the analysis of serum and in observational studies

The developed LC-MS/MS method was applied to the simultaneous measurement of 25OHD$_3$-S and 25OHD$_3$-G in human serum obtained from healthy volunteers. Analysis of 25OHD$_3$ and other vitamin D metabolites in these samples had previously been measured using a prior described LC-MS/MS method (28) Patient demographics of these samples are displayed in Supplemental Table 1. Serum samples from two observational health studies were also used as an application for the LC-MS/MS method to measure 25OHD$_3$-S and 25OHD$_3$-G. Serum samples from a pregnancy cohort were used in which samples were assigned into subgroups based on pregnancy status; non-pregnant females (N-17), first trimester pregnancy (N-24), third trimester pregnancy (N-20), pre-eclampsia (N-21). Data for free vitamin D, including 25OHD$_3$ analysis for these samples has previously been reported (23). Patient demographics of these samples are displayed in Supplemental Table 2. The new LC-MS/MS method was further applied to measuring 25OHD$_3$-S and 25OHD$_3$-G in an observational study consisting of serum samples from females with PCOS (N-9) and a control group of non-PCOS females (N-8). Vitamin D metabolite data including 25OHD$_3$ has been previously measured using a reported LC-MS/MS method for measuring these metabolites in these samples (28). Patient demographics of these samples are displayed in Supplemental Table 3.

3. Results

LC-MS/MS method optimization

The optimized MRM transitions were obtained by running full scan and daughter scan analysis in negative ion mode. The deprotonation of 25OHD$_3$-S and 25OHD$_3$-G gave parent m/z values of 479.4 and 575.4 respectively. Fragmentation of 25OHD$_3$-S gave an abundant sulfate group product ion of m/z 96.9 **(Figure 1a)**, we therefore used the MRM transition of 479.4>96.9 for quantitation. The fragmentation of 25OHD$_3$-G produced multiple transitions with similar intensities **(Figure 1b)**, the abundant fragment 575.4>74.9 was used for quantitation.

Using the chromatographic conditions described in section 2, separation of 25OHD$_3$-S and 25OHD$_3$-G was achieved in a 4.5-minute run time. The retention times for 25OHD$_3$-S and 25OHD$_3$-S-d6 were 2.17 and 2.18 minutes respectively, whilst the retention time for 25OHD$_3$-G was 2.23 minutes.

Method validation

Linearity and calibration curve

Vitamin D depleted serum was used for the preparation of calibration curves. The linearity of each calibration curve was determined by spiking vitamin D depleted serum with nine known concentrations of $25OHD_3$-S (1-200 ng/mL) and $25OHD_3$-G (0.25-25 ng/mL). Calibration curves were plotted as the area ratio of the $25OHD_3$ metabolite to internal standard. Both calibration curves showed good regression coefficients r^2-0.998 $25OHD_3$-S and r^2-0.996 $25OHD_3$-G from three separate calibration curves of each analyte.

Selectivity and LLOQ

The injection of vitamin D depleted serum as a blank matrix confirmed no interfering peaks at the retention times of the analytes (**Figure 2)**. The analysis of a human serum sample by our method confirmed the presence of $25OHD_3$-S and $25OHD_3$-G at the respective retention times the confirmed no matrix interferences directly before or after the respective signals. LLOD levels were determined to be 0.063 ng/mL for $25OHD_3$-S and 0.125 ng/mL for $25OHD_3$-G which produced a signal/noise ratio greater than 3. LLOQ was determined as 0.125 ng/mL for $25OHD_3$-S and 0.250 ng/mL for $25OHD_3$-G which produced a signal/noise ratio greater than 10.

Accuracy and Precision

The method achieved satisfactory accuracy and precision values for both analytes in all QC concentrations. The accuracy and precision values for $25OHD_3$-S and $25OHD_3$-G are summarised in **Table 1.** Intra and inter-day precision, along with accuracy values did not exceed the recommended 15% variation threshold.

Table 1. Precision and accuracy values for $25OHD_3$-S and $25OHD_3$-G at low, medium and high concentrations.

Compound	Concentration (ng/mL)	Level	Precision RSD (%)		Accuracy (%)
			Intra-day N=6+6+6	Inter-day N=18+18+18	
$25OHD_3$-S	2.0	Low	4.8	6.7	107.4

	20	Medium	5.7	6.9	104.6
	100	High	3.2	4.0	101.1
25OHD$_3$-G	0.30	Low	14.9	14.9	99.9
	2.5	Medium	2.6	3.2	108.9
	20	High	6.1	6.8	94.3

Recovery and matrix effects

The absolute recoveries of 25OHD$_3$-S and 25OHD$_3$-G are shown in **Table 2.** The sample preparation procedure yielded recovery rates greater than 90% for 25OHD$_3$-S. The recovery rate was lower for 25OHD$_3$-G, however the achieved recoveries greater than 70% enabled required sensitivity for endogenous quantitation. The matrix effects of both analytes are shown in **Table 2.** There appeared to be no significant signal enhancements or suppression on either 25OHD$_3$-S or 25OHD$_3$-G.

Table 2. Extraction recoveries and matrix effect values for 25OHD$_3$-S and 25OHD$_3$-G at three concentration levels.

Compounds	Concentration (ng/mL), N=6)	Absolute Recovery (%)	Matrix effects (%)
25OHD$_3$-S	2.0	90.9	0.4
	20	99.1	-0.7
	100	94.4	-5.6
25OHD$_3$-G	0.30	83.3	-0.002
	2.50	72.9	-0.012
	20	84.1	-0.051

Application of 25OHD$_3$-S and 25OHD$_3$-G analysis in human serum samples

To assess the application of the method in human serum matrix the method accuracy was determined using four individual human serum samples, by initially measuring the endogenous levels in these samples, and also adding three QC concentrations levels of 25OHD$_3$-S and 25OHD$_3$-G (**Table 3)**. The measured concentrations of 25OHD$_3$-S and 25OHD$_3$-G at each QC level confirmed the accuracy of measurements compared to the expected calculated concentrations. The measured concentrations at each QC level were not over or underestimated

and confirmed the avoidance of matrix effects, or interferences of other endogenous vitamin D metabolites in the analysis of 25OHD$_3$-S and 25OHD$_3$-G in human serum.

Table 3. Baseline measurements and accuracy values post spiking known concentrations of 25OHD$_3$-S and 25OHD$_3$-G in four healthy donor serum samples.

Compounds Sample No.	Baseline measurement (ng/mL)	Calculated (ng/mL)	Measured (ng/mL)	Accuracy (%)	Calculated (ng/mL)	Measured (ng/mL)	Accuracy (%)	Calculated (ng/mL)	Measured (ng/mL)	Accuracy (%)
25OHD$_3$-S		**QCL (2 ng/mL)**			**QCM (20 ng/mL)**			**QCH (100 ng/mL)**		
Donor 1	1.294	3.294	4.058	123.2	21.294	22.623	106.2	101.294	94.297	93.1
Donor 2	19.338	21.338	21.381	100.2	39.338	38.326	97.4	119.338	115.924	97.1
Donor 3	27.603	29.603	29.403	99.3	47.603	45.313	95.2	127.603	128.600	100.8
Donor 4	36.565	38.565	38.747	100.5	56.565	56.651	100.2	136.565	128.390	94.0
25OHD$_3$-G		**QCL (0.3 ng/mL)**			**QCM (2.5 ng/mL)**			**QCH (20 ng/mL)**		
Donor 1	<0.250	0.300	0.295	98.3	2.500	1.967	78.7	20.000	16.282	81.4
Donor 2	3.024	3.324	3.339	100.5	5.524	5.466	99.0	23.024	23.248	101.0
Donor 3	3.823	4.123	4.128	100.1	6.232	6.305	101.2	23.823	24.622	103.4
Donor 4	4.328	4.628	4.652	100.5	6.828	6.917	101.3	24.328	24.336	100.0

The developed LC-MS/MS method was applied to the analysis of serum from 17 healthy human donors to compare concentration ranges of 25OHD$_3$-S and 25OHD$_3$-G, alongside previously measured 25OHD$_3$ (**Figure 3a)**. The measured concentration of 25OHD$_3$-S in these samples was 27.4 ± 11.8 ng/mL (mean ±SD) with measurements ranging between 5.6-49.0 ng/mL. The circulating levels of free 25OHD$_3$ in the same donors (23.8 ± 10.0 ng/mL, 5.5-42.1 ng/mL) had comparable concentrations when compared with 25OHD$_3$-S. The measured 25OHD$_3$-G concentrations were 2.4 ± 1.2 ng/mL (range 0.8-4.2 ng/mL) and approximately 10 times lower than the reported levels of 25OHD$_3$-S and free 25OHD$_3$. In these healthy donors the unconjugated 25OHD$_3$ measurements correlated with both 25OHD$_3$-S (Pearson's correlation coefficient $p<0.001$) and 25OHD$_3$-G (Pearson's correlation coefficient $p=0.006$) (**Figure 3b)** measurements. Increased circulating 25OHD$_3$ will likely elevate the sulfation and glucuronidation of 25OHD$_3$ metabolites owing to increased 25OHD$_3$ available as a substrate for conjugation. However there are still likely to be differences between individuals, owing to interindividual conjugating activities.

Application of the method to determine serum 25OHD$_3$-S and 25OHD$_3$-G in pregnancy

We used out validated analytical method was used to measure 25OHD$_3$-S and 25OHD$_3$-G in human serum from 1st trimester, 3rd trimester and pre-eclampsia pregnancy groups (**Figure 4)**. In these pregnancy sub-groups 25OHD$_3$, 25OHD$_3$-S and 25OHD$_3$-G concentrations were similar across all groups (**Figure 4 A,B,C)**. Measurements of 25OHD$_3$ in these samples had been previously described as having similar levels across pregnancy (23). However, it was

reported that measurements of other free vitamin D metabolites in this study, including the active vitamin D form and catabolite metabolites were significantly ($p<0.05$) higher or lower across pregnancy groups.

In this study, $25OHD_3$-S and $25OHD_3$-G appear to follow the same trend as the unconjugated $25OHD_3$ with no significant increase or decreases in levels observed across pregnancy. By contrast we observed differences in the ratios between $25OHD_3$ metabolites between groups (**Figure 4 D,E,F**). The ratio of $25OHD_3$/$25OHD_3$-S was significantly higher in 3rd trimester pregnancy (1.21 ±0.64 [mean ±SD]), compared with non-pregnant women (0.89 ±0.27, $p<0.05$), and 1st trimester pregnancies (0.80 ±0.30, $p<0.01$). The change in this ratio suggests a shift towards unconjugated $25OHD_3$ over sulfated $25OHD_3$ in 3rd trimester pregnancies, compared with non-pregnant and 1st trimester pregnancies. There were also significant changes observed in the $25OHD_3$-S/$25OHD_3$-G ratio which was lower in 3rd trimester pregnancies (8.32 ±3.28) compared with non-pregnant women (12.39 ±4.65, $p<0.01$) and 1st trimester pregnancies (12.82 ±5.05, $p<0.005$). This suggests there was a shift towards glucuronidation over sulfation in 3rd trimester pregnancies. The ratios between $25OHD_3$/$25OHD_3$-G were not changed across pregnancy.

Previous studies have reported that $25OHD_3$-S and $25OHD_3$-G bind with similar affinities to vitamin D binding protein (DBP) to that of $25OHD_3$ (18). In this study, using previously measured DBP measurements in the 1st, 3rd and PET pregnancy sub-groups (23) we did not observe any association between DBP and concentrations of $25OHD_3$, $25OHD_3$-S or 25OHD-G (**Figure 5)**. The ability of DBP to bind with high affinity to $25OHD_3$-S has been suggested to be an approach to protect the analytes from renal excretion and increase the likelihood of the sulfated form being a reservoir for $25OHD_3$ availability (18). Whilst DBP may play an important role in binding and transporting conjugated $25OHD_3$ metabolites, it does not appear to influence the circulating levels.

Application of the method to determine serum $25OHD_3$-S and $25OHD_3$-G in PCOS

This method, along with a previous analytical method (28) was used to compare unconjugated $25OHD_3$, along with $25OHD_3$-S and $25OHD_3$-G in serum from women with PCOS and healthy control subjects (**Figure 6)**. Directly comparing the concentrations of these three metabolites individually did not show a significant difference in measurements between the PCOS and the healthy control subgroups (**Figure 6 A,B,C).** In addition, there was also no difference in the

ratio of unconjugated 25OHD$_3$/25OHD$_3$-S between groups (**Figure 6 E)**, which suggests that there is no change towards or away from the sulfated form and unconjugated form of 25OHD$_3$ in PCOS. However an increase in the 25OHD$_3$/25OHD$_3$-G and 25OHD$_3$-S/25OHD$_3$-G ratios were observed in the PCOS cohort compared to the healthy control subjects (**Figure 6 F,G)**. These higher ratios suggest a shift towards more of the unconjugated 25OHD$_3$ and 25OHD$_3$-S, with lower glucuronide 25OHD$_3$ in PCOS. Androgen excess is a characteristic of PCOS (29), and studies have described UGT polymorphisms linked with reduced glucuronidation activity in PCOS (30). UGT activity and transcription is reduced with elevated androgens (31, 32) which may in part explain a shift towards less of the glucuronide form of 25OHD$_3$ available.

4. Discussion

A method has been developed and validated by LC-MS/MS to quantify simultaneously circulating 25OHD$_3$-S and 25OHD$_3$-G. The established method enables high throughput analysis of both analytes without requiring derivatization. The Partial LC separation of 25OHD3-S and 25OHD3-G has been described, however this separation could not be extended to achieve complete baseline separation of these analytes. As 25OHD3-S and 25OHD3-G have different *m/z* ratios (479.4 and 575.4 respectively), it has been possible to distinguish between these metabolites based on their optimized MRM transitions, and therefore exclusively measure each of these two analytes separately. Quantitation of 25OHD3-S-d6 internal standard could also be separated from 25OHD3-S owing to the additional six deuterated mass units and having a *m/z* value of 485.4). The development of this method has been applied to understand circulating levels of 25OHD$_3$-S and 25OHD$_3$-G and the comparisons to unconjugated 25OHD$_3$. The LC-MS/MS method described here may have important applications in future clinical studies, to investigate the roles of conjugated 25OHD$_3$ and its biological roles, and possible influences in assessing vitamin D status. This will be particularly important in areas of health that are impacted by vitamin D deficiency, and were impaired and accelerated activities of sulfation or glucuronidation occur.

Here we have shown that 25OHD$_3$-S and 25OHD$_3$-G are present at substantial concentrations in circulation. Also differences between unconjugated and conjugated 25OHD$_3$ in pregnancy and PCOS groups were observed, providing an insight into changes in conjugated vitamin D metabolism. Whilst these metabolites may play an important role in vitamin D metabolism and physiology, differing hypotheses and overlooked information on the role of conjugated vitamin

D metabolites persists. A commonly observed hypothesis for high $25OHD_3$-S levels is that this metabolite acts as a reservoir or storage form of $25OHD_3$ (17, 33). Two pathways have been proposed for $25OHD_3$-S production; sulfation of $25OHD_3$ by SULT2A1, and by hydroxylation of vitamin D_3-S (19, 34). However vitamin D_3-S concentrations in circulation are much lower than $25OHD_3$-S (22), suggesting direct sulfation of $25OHD_3$ as the main pathway in $25OHD_3$-S production. Both $25OHD_3$-S and $25OHD_3$-G bind to and are transported by vitamin D binding protein (DBP), leading to high abundance in circulation and reduced excretion (18). This indicated these metabolites are transported to tissues and cells for local deconjugation to $25OHD_3$, which can be converted to the biologically active $1,25(OH)_2D_3$ (17, 18). However the enzymatic hydrolysis of $25OHD_3$-S or other vitamin D sulfate metabolites has yet to be described (19), so it cannot be confirmed that $25OHD_3$-S is directly de-sulfated locally to $25OHD_3$. Nevertheless, the high throughput protocol for analysis of $25OHD_3$-S described in this manuscript provides a strategy for analysis of this metabolite and its conversion to $25OHD_3$ in specific target tissues. This may be an overlooked but crucial component of the peripheral metabolic pathways required for extra-skeletal effects of vitamin D. Specifically, current mechanisms for effects of vitamin D within settings such as the immune system are based on local, intracrine or paracrine conversion of $25OHD_3$ to $1,25(OH)_2D_3$ (35). Thus, delivery of $25OHD_3$ to cells such as macrophages or dendritic cells is pivotal to vitamin D function in these cells. However, this delivery is impeded by binding to DBP (36), suggesting that it is only the very small fraction of unbound or 'free' $25OHD_3$ that accesses some target cells (37). The potential for some $25OHD_3$ to enter target cells as $25OHD_3$-S may provide a significant alternative pathway for the action of vitamin D within some tissues.

Conjugated forms of $25OHD_3$ may also facilitate responses to vitamin D that are distinct from $25OHD_3$ itself. Both $25OHD_3$-S and $25OHD_3$-G are present in both blood and bile acid and may thus be preferential metabolites for vitamin D function in the gastrointestinal tract (38). In this regard, it is interesting to speculate that enhancement of serum $25OHD_3$ levels using orally administered vitamin D may result in a different conjugated:non-conjugated $25OHD_3$ profile than conventional epidermal production of vitamin D from sunlight exposure. It will be interesting to carry out similar analyses to those described in this manuscript by comparing vitamin D supplemented and placebo supplemented subjects. A different proportion of $25OHD_3$-S or $25OHD_3$–G in subjects receiving supplementary vitamin D could significantly affect the resulting $25OHD_3$ function. There are further applications in which this method could be used in other areas of clinical diagnosis. For example, monitoring changes in sulfated and

glucuronide 25OHD3 levels to identify polymorphisms in SULT2A1 and UGT enzymes. Ultimately this LC-MS/MS method, combined with measurements of unconjugated 25OHD3 could become an important tool in determining vitamin D status, particularly as future studies identify specific clinical areas in which conjugating enzyme activity is increased or decreased.

Conclusion

We have developed and validated a LC-MS/MS method to measure 25OHD3-S and 25OHD3-G and the application of this method has shown the presence of circulating levels of these metabolites in human serum samples. We achieved this by utilizing a solid phase sample preparation method and the optimization of a LC-MS/MS method using negative MRM mode. Conjugated $25OHD_3$ metabolites are likely to play an important role in vitamin D metabolism and physiology owing to high concentrations in circulation and their transportation by DBP. However further investigation is required into the exact mechanisms these metabolites play in circulation and local cells and tissues.

References

1. Holick MF, MacLaughlin JA, Clark MB, Holick SA, Potts JT, Jr., Anderson RR, et al. Photosynthesis of previtamin D3 in human skin and the physiologic consequences. *Science*. 1980;210(4466):203-5.
2. Bikle DD. Vitamin D metabolism, mechanism of action, and clinical applications. *Chem Biol*. 2014;21(3):319-29.
3. Jenkinson C. The vitamin D metabolome: An update on analysis and function. *Cell Biochem Funct*. 2019;37(6):408-23.
4. Cheng JB, Levine MA, Bell NH, Mangelsdorf DJ, Russell DW. Genetic evidence that the human CYP2R1 enzyme is a key vitamin D 25-hydroxylase. *P Natl Acad Sci USA*. 2004;101(20):7711-5.
5. Zhu JG, Ochalek JT, Kaufmann M, Jones G, DeLuca HF. CYP2R1 is a major, but not exclusive, contributor to 25-hydroxyvitamin D production in vivo. *P Natl Acad Sci USA*. 2013;110(39):15650-5.
6. Hollis BW, Horst RL. The assessment of circulating 25(OH)D and 1,25(OH)2D: where we are and where we are going. *J Steroid Biochem Mol Biol*. 2007;103(3-5):473-6.
7. Hollis BW. Circulating 25-hydroxyvitamin D levels indicative of vitamin D sufficiency: implications for establishing a new effective dietary intake recommendation for vitamin D. *The Journal of nutrition*. 2005;135(2):317-22.
8. Adams JS, Hewison M. Extrarenal expression of the 25-hydroxyvitamin D-1-hydroxylase. *Arch Biochem Biophys*. 2012;523(1):95-102.
9. Wang Z, Wong T, Hashizume T, Dickmann LZ, Scian M, Koszewski NJ, et al. Human UGT1A4 and UGT1A3 conjugate 25-hydroxyvitamin D3: metabolite structure, kinetics, inducibility, and interindividual variability. *Endocrinology*. 2014;155(6):2052-63.
10. Kumar R, Nagubandi S, Jardine I, Londowski JM, Bollman S. The isolation and identification of 5,6-trans-25-hydroxyvitamin D3 from the plasma of rats dosed with vitamin D3. Evidence for a novel mechanism in the metabolism of vitamin D3. *J Biol Chem*. 1981;256(18):9389-92.

11. Shimada K, Mitamura K, Saito K, Ohtake Y, Nakatani I. Enzymatic hydrolysis of the conjugate of vitamin D and related compounds. *J Pharm Biomed Anal*. 1997;15(9-10):1207-14.
12. Gao C, Bergagnini-Kolev MC, Liao MZ, Wang Z, Wong T, Calamia JC, et al. Simultaneous quantification of 25-hydroxyvitamin D3-3-sulfate and 25-hydroxyvitamin D3-3-glucuronide in human serum and plasma using liquid chromatography-tandem mass spectrometry coupled with DAPTAD-derivatization. *J Chromatogr B Analyt Technol Biomed Life Sci*. 2017;1060:158-65.
13. Yoshimura Y, Hibi R, Nakata A, Togashi M, Ogawa S, Ishige T, et al. Identification of conjugation positions of urinary glucuronidated vitamin D3 metabolites by LC/ESI-MS/MS after conversion to MS/MS-fragmentable derivatives. *Biomed Chromatogr*. 2019;33(7):e4538.
14. Higashi T, Goto A, Morohashi M, Ogawa S, Komatsu K, Sugiura T, et al. Development and validation of a method for determination of plasma 25-hydroxyvitamin D3 3-sulfate using liquid chromatography/tandem mass spectrometry. *J Chromatogr B Analyt Technol Biomed Life Sci*. 2014;969:230-4.
15. Shimada K, Mitamura K, Kitama N. Quantitative determination of 25-hydroxyvitamin D3 3-sulphate in human plasma using high performance liquid chromatography. *Biomed Chromatogr*. 1995;9(5):229-32.
16. Axelson M, Christensen NJ. Vitamin D metabolism in human pregnancy. Concentrations of free and sulphated 25-hydroxyvitamin D3 in maternal and fetal plasma at term. *J Steroid Biochem*. 1988;31(1):35-9.
17. Foster PA, Mueller JW. SULFATION PATHWAYS: Insights into steroid sulfation and desulfation pathways. *J Mol Endocrinol*. 2018;61(2):T271-T83.
18. Wong T, Wang Z, Chapron BD, Suzuki M, Claw KG, Gao C, et al. Polymorphic Human Sulfotransferase 2A1 Mediates the Formation of 25-Hydroxyvitamin D3-3-O-Sulfate, a Major Circulating Vitamin D Metabolite in Humans. *Drug Metab Dispos*. 2018;46(4):367-79.
19. Kurogi K, Sakakibara Y, Suiko M, Liu MC. Sulfation of vitamin D3 -related compounds-identification and characterization of the responsible human cytosolic sulfotransferases. *FEBS Lett*. 2017;591(16):2417-25.
20. Axelson M. 25-Hydroxyvitamin-D3 3-Sulfate Is a Major Circulating Form of Vitamin-D in Man. *Febs Letters*. 1985;191(2):171-5.
21. Higashi T, Yokota M, Goto A, Komatsu K, Sugiura T, Ogawa S, et al. A Method for Simultaneous Determination of 25-Hydroxyvitamin D3 and Its 3-Sulfate in Newborn Plasma by LC/ESI-MS/MS after Derivatization with a Proton-Affinitive Cookson-Type Reagent. *Mass Spectrom (Tokyo)*. 2016;5(Spec Iss):S0051.
22. Gomes FP, Shaw PN, Hewavitharana AK. Determination of four sulfated vitamin D compounds in human biological fluids by liquid chromatography-tandem mass spectrometry. *J Chromatogr B Analyt Technol Biomed Life Sci*. 2016;1009-1010:80-6.
23. Tamblyn JA, Susarla R, Jenkinson C, Jeffery LE, Ohizua O, Chun RF, et al. Dysregulation of maternal and placental vitamin D metabolism in preeclampsia. *Placenta*. 2017;50:70-7.
24. Butts SF, Seifer DB, Koelper N, Senapati S, Sammel MD, Hoofnagle AN, et al. Vitamin D Deficiency Is Associated With Poor Ovarian Stimulation Outcome in PCOS but Not Unexplained Infertility. *The Journal of clinical endocrinology and metabolism*. 2019;104(2):369-78.
25. O'Reilly MW, Kempegowda P, Walsh M, Taylor AE, Manolopoulos KN, Allwood JW, et al. AKR1C3-Mediated Adipose Androgen Generation Drives Lipotoxicity in Women With Polycystic Ovary Syndrome. *J Clin Endocrinol Metab*. 2017;102(9):3327-39.
26. Rotterdam EA-SPCWG. Revised 2003 consensus on diagnostic criteria and long-term health risks related to polycystic ovary syndrome. *Fertility and sterility*. 2004;81(1):19-25.
27. Administration UFaD. Bioanalytical Method Validation Guidance for Industry 2018 [2018:[Available from: https://www.fda.gov/regulatory-information/search-fda-guidance-documents/bioanalytical-method-validation-guidance-industry.

28. Jenkinson C, Taylor AE, Hassan-Smith ZK, Adams JS, Stewart PM, Hewison M, et al. High throughput LC-MS/MS method for the simultaneous analysis of multiple vitamin D analytes in serum. *J Chromatogr B Analyt Technol Biomed Life Sci*. 2016;1014:56-63.
29. O'Reilly MW, Kempegowda P, Jenkinson C, Taylor AE, Quanson JL, Storbeck KH, et al. 11-Oxygenated C19 Steroids Are the Predominant Androgens in Polycystic Ovary Syndrome. *The Journal of clinical endocrinology and metabolism*. 2017;102(3):840-8.
30. Luo Y, Nie Y, Tang L, Xu CC, Xu L. The correlation between UDP-glucuronosyltransferase polymorphisms and environmental endocrine disruptors levels in polycystic ovary syndrome patients. *Medicine (Baltimore)*. 2020;99(11):e19444.
31. Barrett ES, Sobolewski M. Polycystic ovary syndrome: do endocrine-disrupting chemicals play a role? *Semin Reprod Med*. 2014;32(3):166-76.
32. Takeuchi T, Tsutsumi O, Ikezuki Y, Kamei Y, Osuga Y, Fujiwara T, et al. Elevated serum bisphenol A levels under hyperandrogenic conditions may be caused by decreased UDP-glucuronosyltransferase activity. *Endocr J*. 2006;53(4):485-91.
33. Higashi T, Shimada K, Toyo'oka T. Advances in determination of vitamin D related compounds in biological samples using liquid chromatography-mass spectrometry: a review. *J Chromatogr B Analyt Technol Biomed Life Sci*. 2010;878(20):1654-61.
34. Yoshimura Y, Togashi M, Ogawa S, Higashi T. 3-Epi-25-hydroxyvitamin D3 is a poor substrate for SULT2A1: Analysis of its 3-sulfate in cord plasma and recombinant human SULT2A1 incubate. *Steroids*. 2020;162:108695.
35. Hewison M. Vitamin D and immune function: autocrine, paracrine or endocrine? *Scand J Clin Lab Invest Suppl*. 2012;243:92-102.
36. Chun RF, Lauridsen AL, Suon L, Zella LA, Pike JW, Modlin RL, et al. Vitamin D-binding protein directs monocyte responses to 25-hydroxy- and 1,25-dihydroxyvitamin D. *The Journal of clinical endocrinology and metabolism*. 2010;95(7):3368-76.
37. Chun RF, Peercy BE, Orwoll ES, Nielson CM, Adams JS, Hewison M. Vitamin D and DBP: the free hormone hypothesis revisited. *J Steroid Biochem Mol Biol*. 2014;144 Pt A:132-7.
38. Gao C, Liao MZ, Han LW, Thummel KE, Mao Q. Hepatic Transport of 25-Hydroxyvitamin D3 Conjugates: A Mechanism of 25-Hydroxyvitamin D3 Delivery to the Intestinal Tract. *Drug Metab Dispos*. 2018;46(5):581-91.

Legends to figures

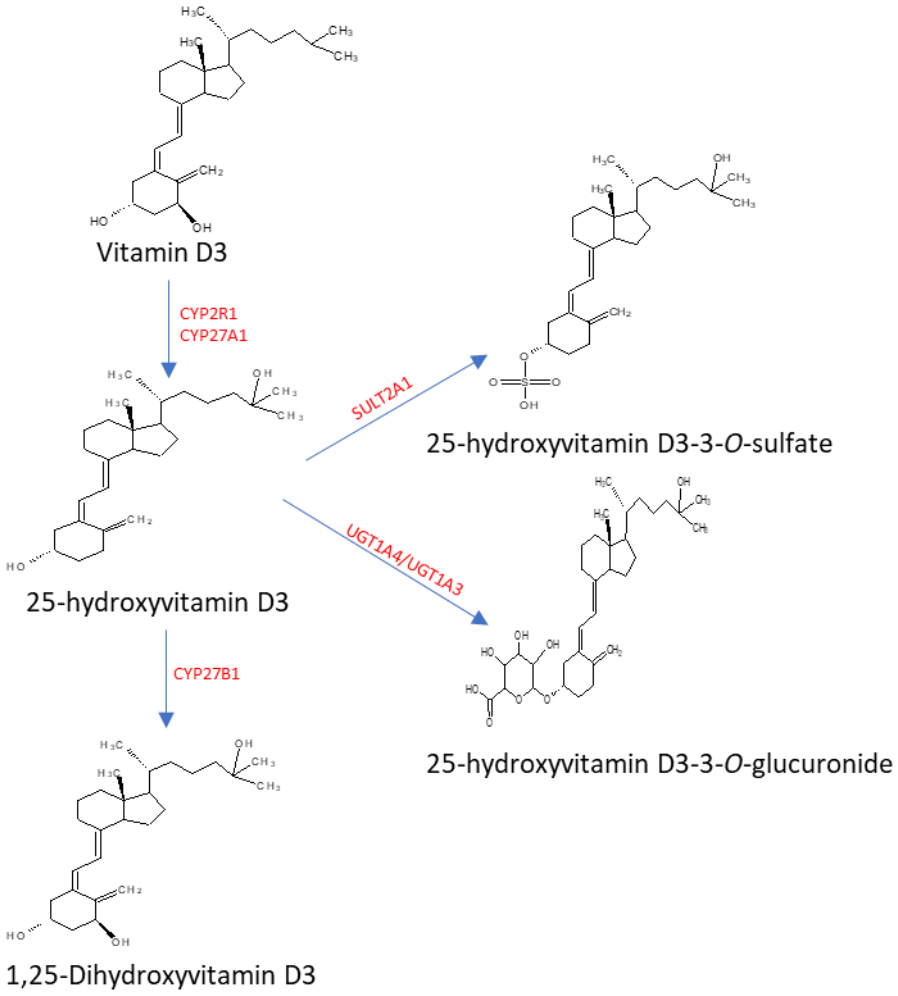

Figure 1: Pathway for the activation of vitamin D3 to $1,25(OH)_2D3$ and the conjugation pathways for the sulfation and glucuronidation of 25OHD3. The structures of each metabolite in the pathway are also displayed

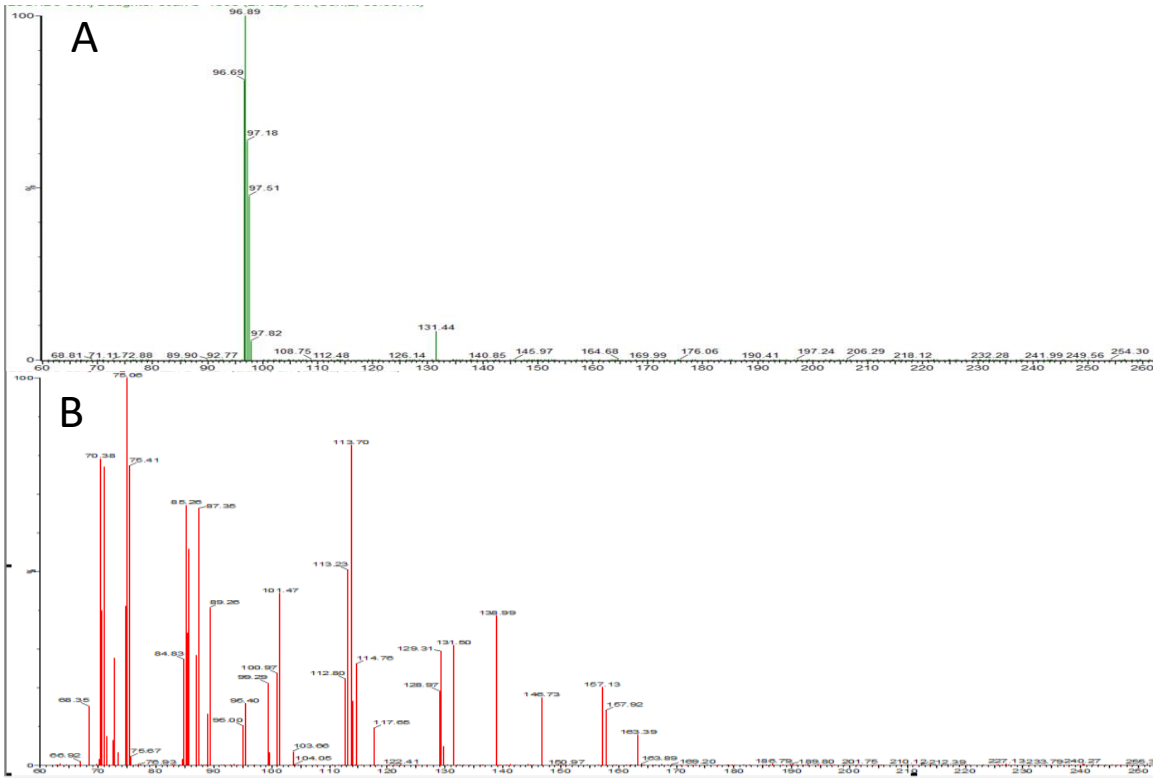

Figure 2: Product ion spectra of **A**-25OHD$_3$-S and **B**-25OHD$_3$-G in negative mode, under the MS conditions described in section two, running a collision energy range between 20-60 V.

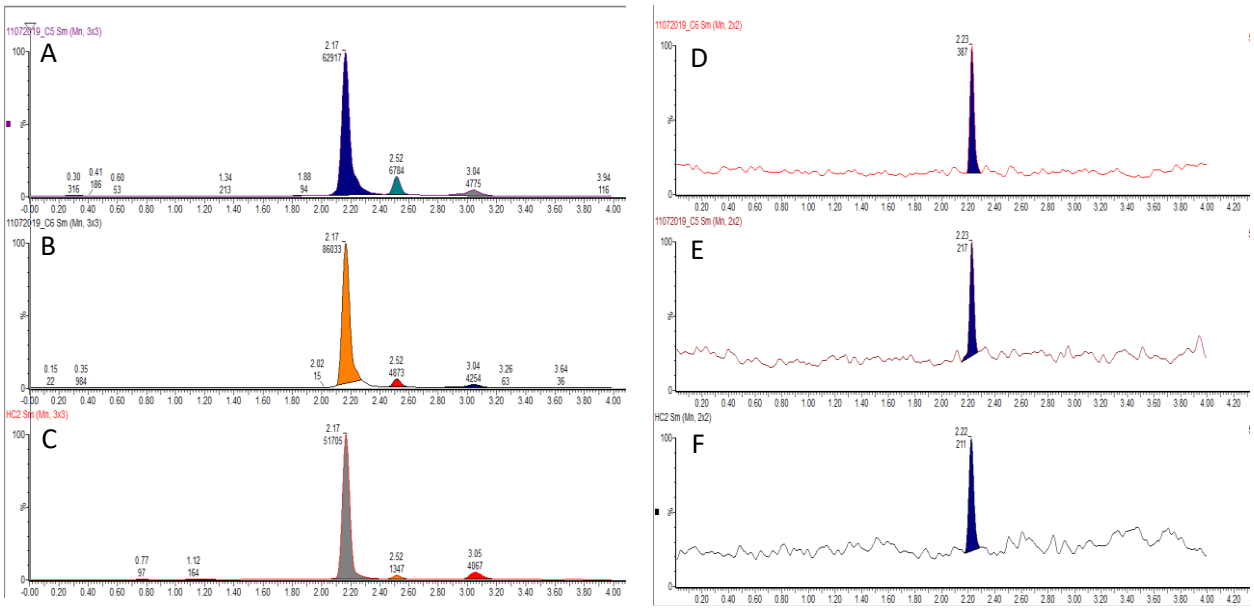

Figure 3: MRM chromatograms of 25OHD$_3$ conjugate metabolites including 25OHD$_3$-S extracted from vitamin D depleted serum spiked with 16 ng/mL (2A) and 32 ng/mL (2B) 25OHD$_3$-S, along with an extracted human serum sample (2C). MRM chromatograms of 25OHD$_3$-G show samples of vitamin D depleted serum extracted, spiked with 2 ng/mL (2A) and 4 ng/mL (2B) 25OHD$_3$-G, along with an extracted human serum sample (2C). The retention times of 25OHD$_3$-S and 25OHD$_3$-G were confirmed by spiking 16 and 32 ng/mL 25OHD$_3$-S, and 0.5 and 1 ng/mL 25OHD$_3$-G in vitamin D depleted serum

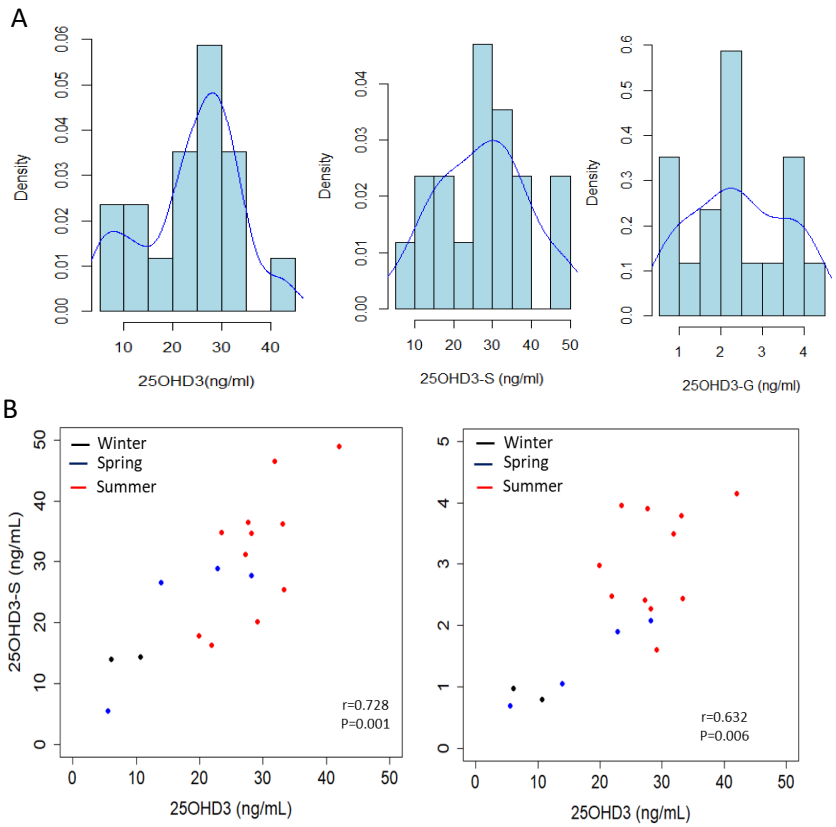

Figure 4: A- Concertation ranges of $25OHD_3$, $25OHD_3$-S and $25OHD_3$-G measured in healthy control donor serums. **B-** Correlations between the unconjugated $25OHD_3$ and $25OHD_3$-S, and unconjugated $25OHD_3$ and $25OHD_3$-G in healthy individuals, according to season of sample collection.

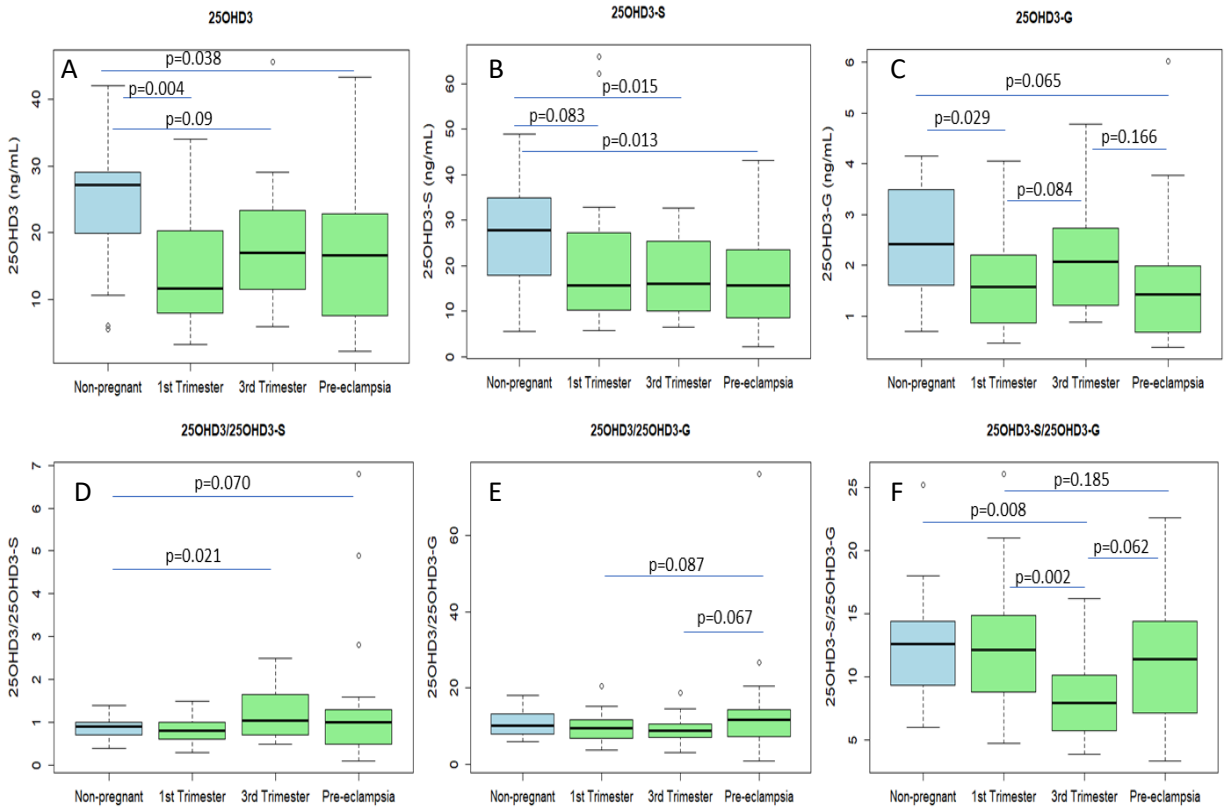

Figure 5: Serum concentrations of **A**-25OHD$_3$, **B**-25OHD$_3$-S and **C**-25OHD$_3$-G in pregnant and non-pregnant women, along with ratios between 25OHD$_3$ metabolites; **D**-25OHD$_3$/25OHD$_3$-S, **E**-25OHD$_3$/25OHD$_3$-G and **F**-25OHD$_3$-S/25OHD$_3$/G.

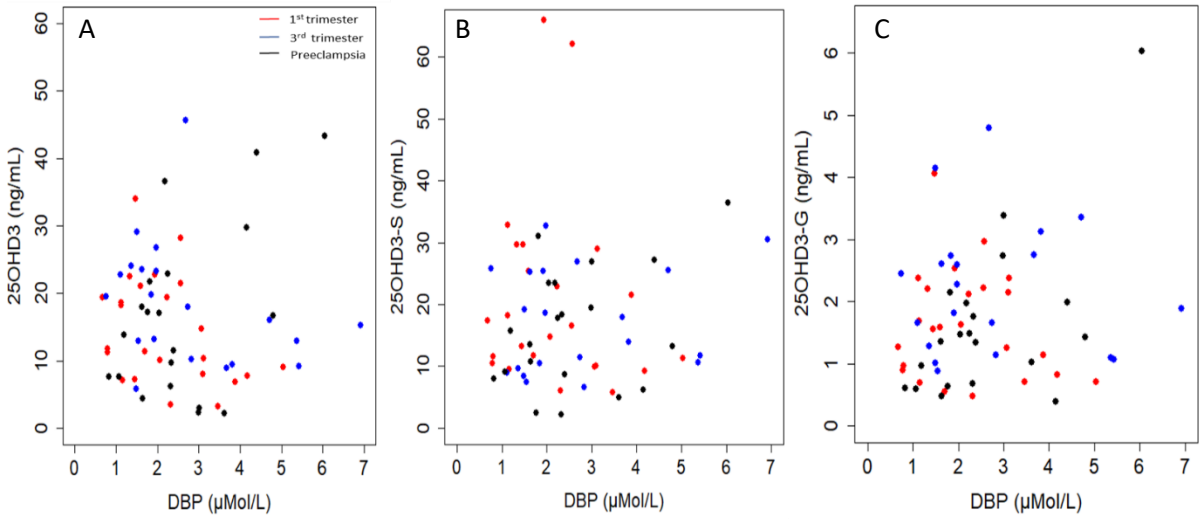

Figure 6: Effect of DBP on serum 25OHD$_3$ concentrations. Serum concentrations of **A-**25OHD$_3$, **B-**25OHD$_3$-S and **C-**25OHD$_3$-G were correlated with DBP concentrations in 1st trimester, 3rd trimester and pre-eclampsia samples.

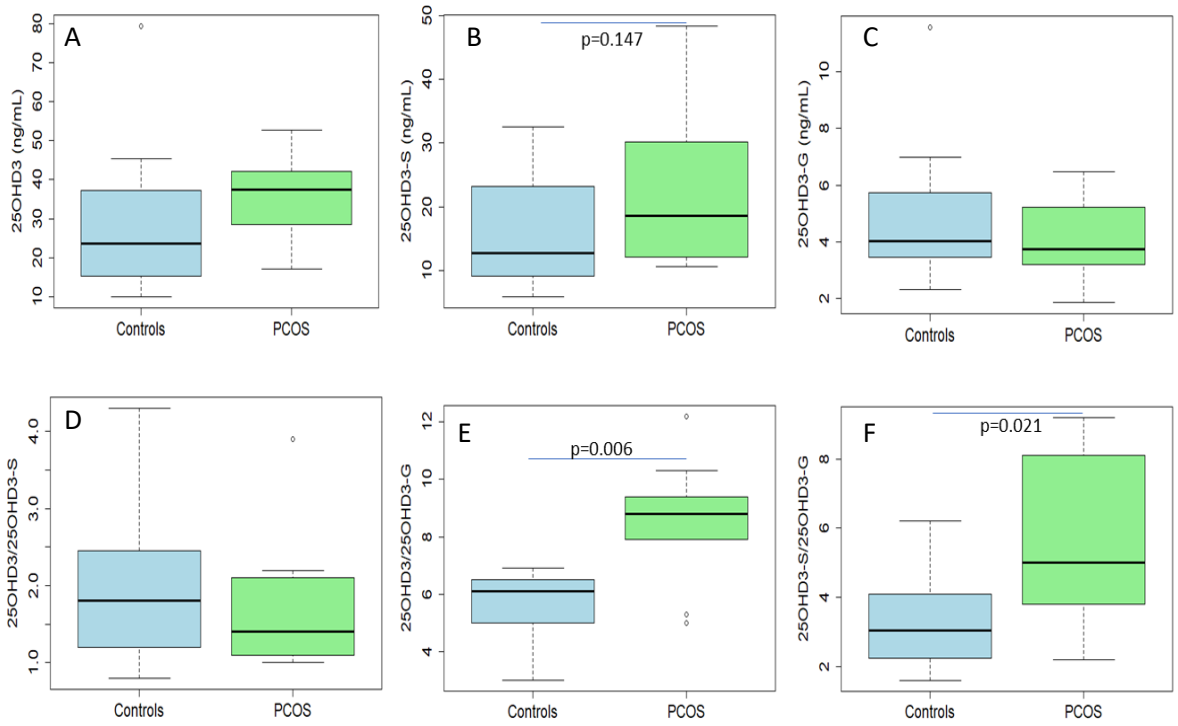

Figure 7: Serum concentrations of **A**-25OHD$_3$, **B**-25OHD$_3$-S and **C**-25OHD$_3$-G in women with PCOS and healthy matched female control subjects, along with along with ratios between 25OHD$_3$ metabolites; **D**-25OHD$_3$/25OHD$_3$-S, **E**-25OHD$_3$/25OHD$_3$-G and **F**-25OHD$_3$-S/25OHD$_3$-G.